Photic and non-photic modulation of the mammalian circadian clock

Oosterhout, F.F.T.O. van

[1.] Laboratory for Neurophysiology, Department of Molecular Cell Biology,
Leiden University Medical Centre, Leiden, The Netherlands

[2.] Nuffield Laboratory of Ophthalmology, Nuffield Department of Clinical Neurosciences
University of Oxford, John Radcliffe Hospital, Oxford, UK

CHAPTER 4

Ultraviolet light provides a major input to the circadian system in mice

Current Biology, ***under revision***

Floor van Oosterhout[1], Simon P. Fisher[2], Hester C. van Diepen[1], Thomas S. Watson[2], Thijs Houben[1], Henk Tjebbe VanderLeest[1], Stewart Thompson[3], Stuart N. Peirson[2], Russell G. Foster[2], Johanna H. Meijer[1]

ABSTRACT

The change in irradiance at dawn and dusk provides the primary cue for the entrainment of the mammalian circadian pacemaker to the 24h day. Irradiance detection has been ascribed largely to melanopsin-based phototransduction (Berson et al., 2002; Drouyer et al., 2007; Mure et al., 2007; Gooley et al., 2010; Brown et al., 2011). Here we examine the role of ultraviolet sensitive (UVS) cones in the modulation of circadian behaviour, sleep, and suprachiasmatic nuclei (SCN) electrical activity. Ultraviolet (UV) light exposure leads to phase shifting responses similar to those induced by visible light. Moreover, UV light exposure induces sleep in wildtype and melanopsin-deficient (*Opn4*$^{-/-}$) mice with equal efficacy. Electrical recordings from the SCN of wildtype mice reveal that UV light elicits irradiance-dependent sustained responses that are similar to those induced by white light, with characteristic fast-transient components occurring at the light transitions. These responses were retained in *Opn4*$^{-/-}$ mice and, unexpectedly, they were preserved under saturating photopic conditions. The sensitivity of phase-shifting responses to UV light is unaffected by the loss of rods, but severely attenuated by loss of rods and cones. Our data suggest that UVS cones have an important role in circadian and sleep regulation in mice.

RESULTS AND DISCUSSION

Behavioural responses to UV light

We assessed the phase shifting effects of UV light on circadian wheel running activity (**Figure 1A-C**). We found that wildtype mice show a robust response to UV light **(Figure 1A)**. A phase response curve to UV light (UV LED, 12.9 log quanta/cm^2/s; 45 min) was constructed from 41 data points that were obtained from 24 mice (**Figure 1B**). Mean shifts ± SEM for data pooled in three-hourly bins showed significant differences over time ($p < 0.05$). Phase delays observed during the early subjective night reached on average -127±11 min at around CT15 (CT15 ± 1.5h; n=8; $p < 0.05$). Small, but significant advances occurred in the late subjective night at around CT21 (mean shift ± SEM at CT21 ± 1.5h = 29 ± 8 min; n=5; $p < 0.05$). No effect of UV light was found during the subjective day (CT0-CT12, $p > 0.05$). These phase delays and small advances mirror the phase-response curve (PRC) for white light in C57BL/6 mice (Pittendrigh and Daan, 1976; Vanderleest et al., 2009) and of UV light in the field mouse (Sharma et al., 1998).

The effect of light pulse duration on the magnitude of phase shifts in wheel running activity was investigated at the time of maximal delays (CT14-16; **Figure 1C**). Pulses of up to 10 sec appeared ineffective to induce significant phase shifts (2 sec: 6.8 ± 2.3 min; 10 sec: 15.3 ± 4.4 min, $p > 0.05$). Following 100 sec pulses, the phase of wheel running activity onset was significantly delayed (29.6 ± 10.9 min, $p < 0.05$). With increasing stimulus duration, a significant increase in phase delay magnitude was observed. In response to 1000, 2700, and 10,000 sec light pulses, phase delays of 84.3 ± 8.2 min ($p < 0.05$), 134.0 ± 14.1 min ($p < 0.01$), and 168.5 ± 8.0 min ($p < 0.01$) were found, respectively. The duration response curve was fitted with a sigmoid function using the method of least squares ($R^2 = 0.998$). These results show that the circadian system is capable of integrating UV light in a manner that is comparable to light in the visible spectrum (Pittendrigh and Daan, 1976; Nelson and Takahashi, 1999). This is consistent with earlier reports that UV light can act as an important stimulus for the regulation of circadian behavior (Provencio and Foster, 1995; Von Schantz et al., 1997; Sharma et al., 1998; 2000; Amir and Robinson, 1995; Hut et al., 2000), pupil light reflex (Allen et al., 2011) and neuroendocrine responses in rodents (Benshoff et al., 1987; Podolin et al., 1987; Brainard et al., 1994).

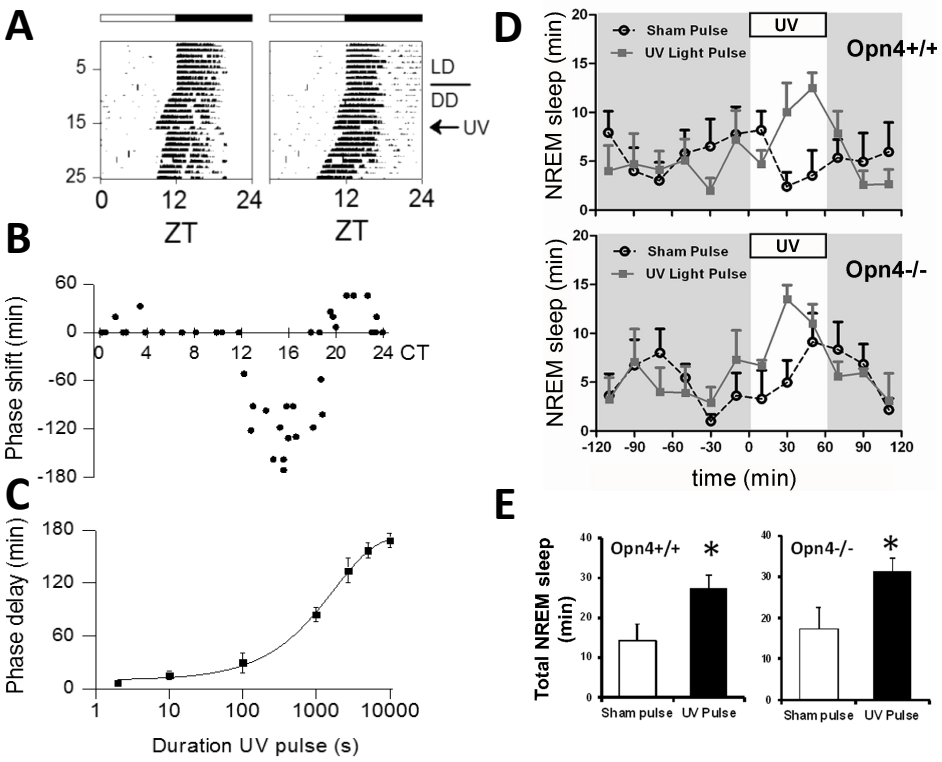

Figure 1. Behavioural and NREM sleep responses to UV light. (A) Representative actograms showing the phase shifting response of wheel running activity to UV light in C57Bl/6 mice. UV light pulses were applied on the 7th day in DD (CT15). **(B)** Phase response curve of wheel running activity to UV light pulses (365nm, 12.9 log quanta/cm^2/s, 45min exposure). Phase shift magnitude and direction are plotted as a function of the circadian time. **(C)** Duration effects of phase shifts in response to UV light exposure at CT16 (365nm, 12.9 log quanta/cm^2/s). Phase shifts are duration-dependent, increasing in magnitude with longer light exposure as has been previously shown for white light. **(D)** Time course of NREM sleep following UV light exposure, showing responses in Opn4$^{+/+}$ and Opn4$^{-/-}$ mice (n=5). **(E)** Histograms summarizing changes in NREM sleep in response to UV light exposure. UV light administered at ZT 16-17 results in a significant increase of NREM sleep in Opn4$^{+/+}$ mice, and a significant increase sleep in Opn4$^{-/-}$ mice. * indicates P<0.05.

UV light induces sleep in *Opn4*$^{+/+}$ and *Opn4*$^{-/-}$ mice

In view of our findings that UV light can fully replicate melanopsin mediated light responses at the level of circadian behaviour, we examined the contribution of UV light to the acute regulation of sleep. In *Opn4*$^{+/+}$ mice (n=5), a UV light pulse increased the amount of non-REM (NREM) sleep by 93% (**Figure 1D, E**). The same UV light pulse administered to *Opn4*$^{-/-}$ mice (n=5) also significantly increased NREM sleep by

79%. A UV light pulse was also found to increase the amount of REM by 166% in *Opn4*$^{+/+}$ mice and by 98% in *Opn4*$^{-/-}$ mice, but this increase was not statistically significant (**Figure S1**). Our results showed that UV light was as effective as white light in inducing sleep in mice (Lupi et al., 2008) and that in the absence of melanopsin there was no attenuation of UV induced sleep compared to *Opn4*$^{+/+}$ mice.

Recent studies have demonstrated that melanopsin plays a dominant role in regulating the acute effects of white light on sleep induction (Lupi et al., 2008; Tsai et al., 2009). An additional study, using somewhat different methodologies, showed that in response to broad-spectrum white light *Opn4*$^{-/-}$ mice show a transient induction of sleep, but then fail to show sustained sleep (Altimus et al., 2008). In the same study, mice which lack functional rods and cones ("melanopsin-only" mice; *Gnat1*$^{-/-}$;*Cnga3*$^{-/-}$) showed sleep induction that was sustained for 30 minutes. Collectively these data suggested that melanopsin provides the major channel for the induction of sleep. The present study is the first to demonstrate that UV light exposure induces sleep in mammals during their habitual wake period, and suggests that UV irradiance detection may be an important feature of additional non-image forming responses to light in mice.

SCN electrical activity

Firing frequencies of populations of SCN neurons were recorded in freely moving animals to characterize the response pattern to monochromatic UV light. Animals that showed a clear rhythm in SCN electrical activity, with high discharge rate during the day and low discharge rate during the night, were examined for the presence of responses to white light (**Figure 2A**). Light-induced SCN responses were shown in a minority of 7 out of 24 mice (34%), all of which were also sensitive to UV light. Not all individual SCN neurons showed responses to light (**Figure S2**), which is consistent with previous studies showing that broad spectrum white light fails to activate all SCN neurons (Groos and Mason, 1980; Meijer et al., 1986). Photic stimulation with pulses of 365nm light induced an increase in the SCN electrical discharge pattern (**Figure 2A**). Typically, the UV-light- activated response started with a transient overshoot response at lights on ("on-excitation"). During light exposure, electrical activity levels were elevated compared to baseline levels and the increased firing rate was maintained over the course of the light pulse. At lights off, a fast transient drop ("off- inhibition") in SCN activity was observed, which gradually returned to baseline

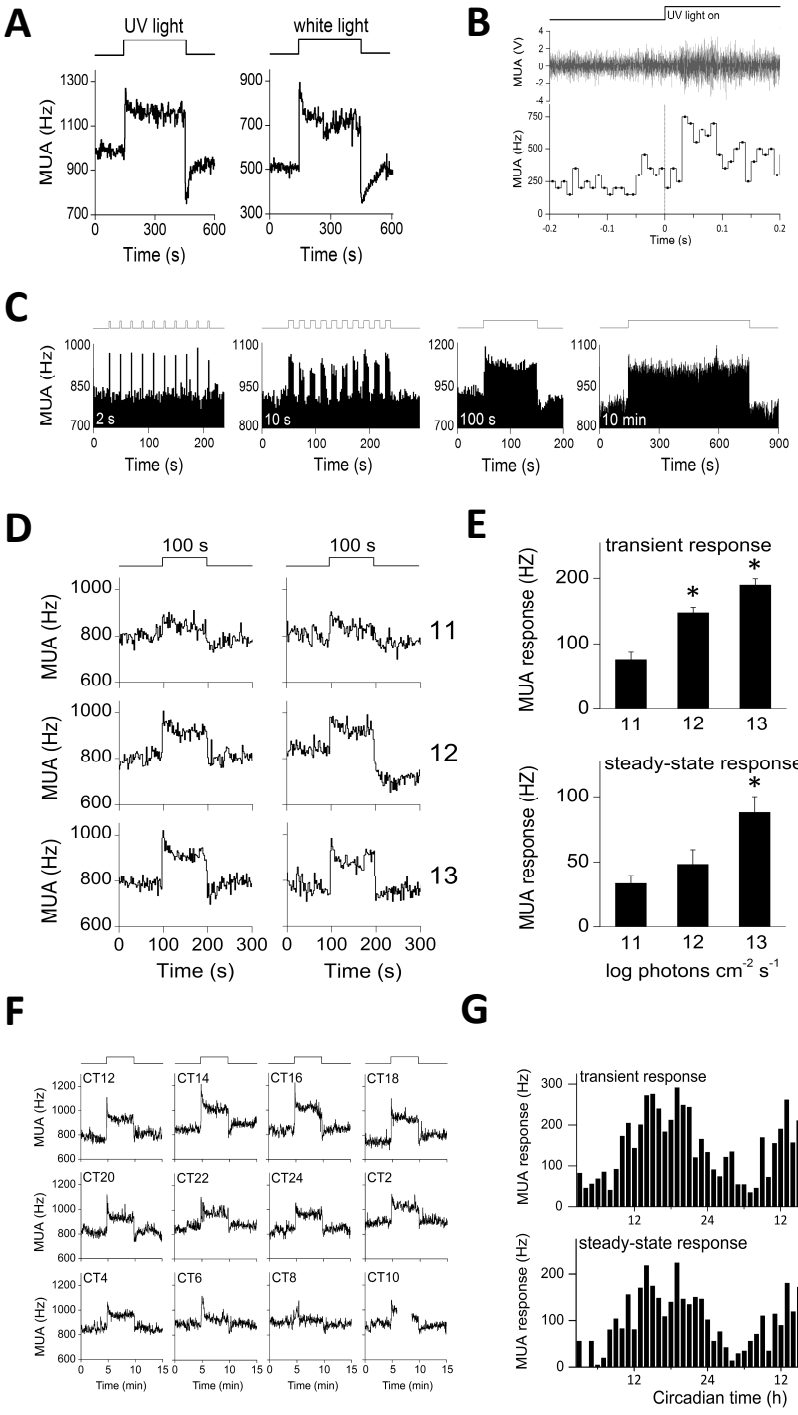
A
UV light
white light
MUA (Hz)
Time (s)
B
UV light on
MUA (V)
MUA (Hz)
Time (s)
C
MUA (Hz)
2 s
10 s
100 s
10 min
Time (s)
D
100 s
100 s
MUA (Hz)
11
12
13
Time (s)
E
transient response
MUA response (HZ)
steady-state response
MUA response (HZ)
log photons cm-2 s-1
F
CT12
CT14
CT16
CT18
CT20
CT22
CT24
CT2
CT4
CT6
CT8
CT10
MUA (Hz)
Time (min)
G
transient response
steady-state response
MUA response (Hz)
Circadian time (h)

Figure 2. SCN electrical activity responses to UV light in freely-moving mice. (A) Representative SCN multiunit activity (MUA) responses to a 5-min UV light or white light pulse. MUA responses to UV light typically show a fast transient increase in spike frequency to lights on, a sustained response during light exposure and a fast transient decrease at lights off. Bin size = 2s. **(B)** Response latency to UV light. Time of lights on is indicated by the step diagram. Upper graph shows a representative trace of multiunit activity in the SCN, with spike frequency above threshold shown in the lower graph (bin size = 0.01s). Vertical line indicates the time of UV onset (t = 0). SCN firing rate is increased in response to UV light, with a latency of 0.04s. **(C)** MUA responses to UV light pulses of different durations, applied between CT14-CT16. From left to right: 2s lights on, 18s lights off (10x); 10s lights on, 10s lights off (10x); 100s lights on; 10min lights on. Stimulus presentation is indicated by the step diagram above each plot. **(D)** Representative traces of SCN electrical activity to 100s UV light pulses of different irradiances. Two examples are shown for each irradiance level. Log quanta/cm^2/s is indicated on the right. **(E)** Summary of MUA response magnitude as a function of UV irradiance (11, 12, and 13 log quanta/cm^2/s with n=8; n=8; n=7, respectively). Upper graph shows the difference in spike frequencies between the transient response and baseline for the three irradiance levels. Lower graph shows the difference in spike frequency between steady state level and baseline level, for the three irradiance levels. Both transient and steady-state responses show irradiance-dependent effects. **(F)** Examples of SCN responses to 5-min UV light pulses at different times of the circadian cycle. **(G)** Off-line analysis shows a clear circadian rhythm in transient "on-response" magnitude (upper graph) and in steady-state response magnitude (lower graph). For transient responses, the difference in spike frequency between the transient response (determined by the first data point after lights on) and baseline level (calculated from the average of the last 120 sec before lights on) was plotted versus circadian time over 48h. For steady state responses, the difference in spike frequency between the steady state level (calculated from the average of the last 240s of the 300s light pulse) and baseline level was plotted versus circadian time over 48h.

levels. Analyses of the response kinetics revealed that the UV-light-induced response has a short latency of 30-40 msec (n=30) following lights on (**Figure 2B**).

We found highly elevated SCN discharge rates in response to UV light pulses as brief as 2 sec (**Figure 2C**), consistent with studies showing chromatic sensitivity to flashes of light (0.1 – 1 sec) (Aggelopoulos and Meissl, 2000). Interestingly, with increasing stimulus durations, i.e. 10 sec, 100 sec and up to 10 minutes, activated SCN cell populations maintained increased firing frequencies for the full duration of the light presentation. The influence of irradiance on SCN electrical activity levels was investigated by application of 100-sec UV light pulses with different irradiance levels ranging over 3 log units (11-13 log quanta/cm^2/s, n=7-8; **Figure 2D**). Increased stimulus irradiance resulted in more than a two-fold increase in SCN firing response. Both the magnitudes of the transient on-excitation response and the steady-state response were shown to be irradiance-dependent (11 vs. 13 log quanta/cm^2/s; $p < 0.05$; **Figure 2E**).

To determine the effect of circadian phase on UV light responses, three mice were exposed to hourly 5 min UV light pulses over 24h (n=1) or 48h (n=2) (**Figure 2F**). Analyses of the on-excitation response magnitude as well as the steady-state response magnitude over time showed a clear phase-dependent sensitivity of SCN electrical activity to UV light pulses, with relative small responses during the day and large responses during the night (**Figure 2G**). Such time-of-day effects have also been reported for white light (Meijer et al., 1998). Despite the responsiveness of the SCN to UV light during the subjective day (**Figure 2F,G**), no behavioral phase shifts are induced at this phase of the cycle (see PRC in **Figure 1B**). This is consistent with the view that the signaling pathway mediating behavioral phase shifts is a post-synaptic event, downstream from the recorded membrane event (Meijer et al., 1998).

UV light responses in *Opn4*$^{-/-}$ mice

We investigated whether the sustained UV light induced firing response of SCN neurons was retained in melanopsin-deficient mice (*Opn4*$^{-/-}$). Successful implantations of micro-electrodes aimed at the ventral SCN were performed in 4 *Opn4*$^{-/-}$ mice and 2 *Opn4*$^{+/+}$ controls, all of which were responsive to UV light. SCN firing frequencies increased in response to UV light pulses (365nm) of all durations tested (2 s, 10 s, 100 s, 10 min) **(Figure S3)**. The firing pattern showed similar kinetics as described in detail for C57BL/6 mice: fast transient "on-excitation" and "off-inhibition" responses, with an onset latency of 30-40 msec (n = 27); and persistence of the increased electrical discharge throughout the duration of the light pulse **(Figure 3A)**. The magnitude of the transient on-excitation response as well as the steady-state response were irradiance dependent (11 - 13 log quanta/cm^2/s, n=4-7, **Figure 3B,C**), showing significantly increased magnitude with increased irradiance (11 vs. 13 log quanta/cm^2/s; $p < 0.05$). These results are consistent with our observation that UV light is capable of evoking phase shifts in *Opn4*$^{-/-}$ mice that are indistinguishable from those seen in wildtype littermate controls (**Figure S4**).

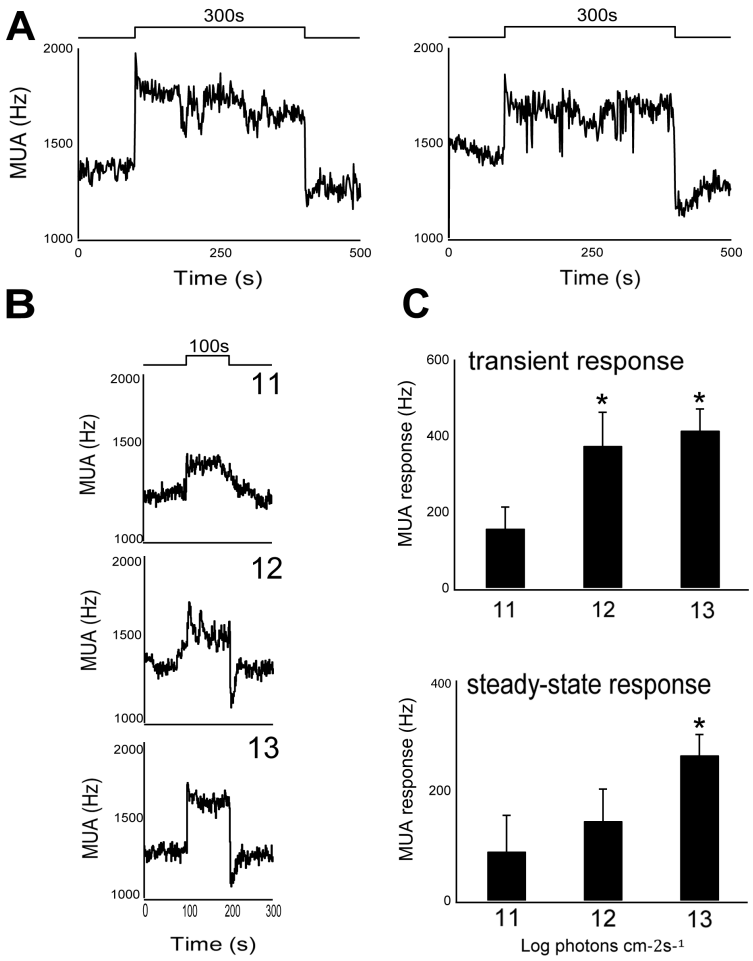

Figure 3. Responses to UV light in melanopsin-deficient mice (A) Two representative traces of SCN multiunit activity (MUA) in response to 5 min UV light exposure in *Opn4*$^{-/-}$ mice. MUA responses to UV light typically show a fast transient increase in spike frequency to lights on, a sustained response during light exposure and a fast transient decrease at lights off. Bin size is 2s. **(B)** Electrical responses to 100s UV light exposure at three different irradiances (one representative trace is shown per irradiance, with log quanta/cm^2/s shown on the right). **(C)** Histograms showing mean MUA responses as a function of UV irradiance (11, 12 and 13 log quanta/cm^2/s, n=4-7 per irradiance). Upper graph shows changes in spike frequency between baseline levels and the transient response against irradiance. Lower graph shows changes in spike frequency between baseline levels and the steady-state level against irradiance. Both transient and steady-state responses show irradiance dependent effects.

Importantly, the present results indicate that the persistent UV-driven SCN response can occur independently from melanopsin-based phototransduction. The question we now have to address is how? The SCN receives photic input solely from a small population of melanopsin-expressing retinal ganglion cells (pRGCs) (Goz et al., 2008; Guler et al., 2008; Hatori et al., 2008), which are intrinsically photosensitive (Berson et al., 2002; Sekaran et al., 2003), but are also innervated extrinsically by the indirect synaptic input from rod and cone photoreceptors (Belenky et al., 2003; Dacey et al., 2005; Wong et al., 2007; Schmidt and Kofuji, 2010). The presently observed very short latencies are in close agreement with those previously shown for cone-mediated fast reaction times measured from pRGCs (30-40ms [Dacey et al., 2005]; 50-60ms [Wong et al., 2007]), and differ from both rod-mediated response latencies (150ms [Dacey et al., 2005]) and melanopsin-mediated response latencies (>300ms to minutes [Berson et al., 2002; Sekaran et al., 2003; Dacey et al., 2005). This result implicates the involvement of cones.

The most parsimonious explanation for the observed UV photosensitivity is that it is mediated by UVS cones. However, under the currently used conditions of dark adaptation, we cannot exclude that the sustained component of the response may rely on additional rod activation (Altimus et al, 2010; Lall et al., 2010). To test the hypothesis that the UV photosensitivity is mediated by UVS cones, we measured the SCN neuronal response to UV light in the presence of a broad spectrum white light background. We used a high-power incandescent light source that emitted a continuous spectrum with a cut-off at 400nm, which was designed to maximally stimulate rods and LWS cones. By recordings of a series of SCN responses to different levels of light, using neutral density filters, we verified that the light stimulus induced saturating responses of SCN neuronal activity. Under these photopic conditions, additional (long-wavelength) light failed to induce further increments of the electrical discharge rates. Strikingly, when UV light pulses were applied, clear light responses were elicited on top of the white light-induced response (**Figure 4**), which showed both transients and sustained components.

Our results show that UV light can elicit transient and sustained responses to light within the SCN. The high sensitivity to UV light both under scotopic and photopic conditions, the short response latency to UV light, the behavioural UV light responses in animals deficient of rods (Provencio and Foster, 1995; this study) or melanopsin (this study), all add to the hypothesis that the UV-light induced effects have their origin predominantly from UVS cones. We propose that the UVS cone participates in

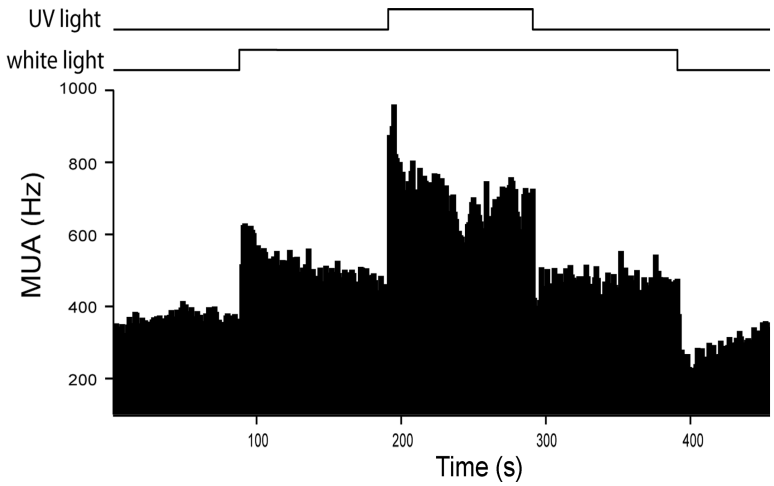

Figure 4. SCN neuronal response to UV light under photopic light conditions in a wild-type mouse. An excitatory response of the SCN electrical discharge rate is induced by exposure to saturating white light. After 100 seconds, a 100-s UV light pulse is applied, which evokes a further increment of the SCN firing rate. The light protocol is indicated by the bars above the graph.

pRGC synaptic signaling. Additional support for this hypothesis comes from recent results showing that pRGCs retain the capability of a tonic response in the absence of melanopsin but in the presence of an intact synaptic input from rods and cones (Schmidt and Kofuji, 2010). The capacity to encode steady-state irradiance could be a special property of murine UVS cone photoreceptors; or perhaps a response of pRGCs to UVS cone input; or even a dedicated input by UVS cones to a specialized sub-set of pRGCs. The current findings suggest that UVS cones function as an integrated part of the circadian system in encoding ambient irradiance levels.

Phase-shifting responses to UV light are cone-dependent

To confirm the identity of the photoreceptor responsible for the UV responses we describe, we conducted a series of phase-shifting experiments in retinal transgenics. We first determined that the UV sensitivity of wildtype mice, as determined by action spectroscopy based upon 8 monochromatic wavelengths (**Figure S5**), is comparable to peak sensitivity (**Figure 5A**). Comparison of UV irradiance response curves (365nm LED stimulus) show that mice lacking rods (*rd/rd*) do not differ in sensitivity from wildtype controls, but mice lacking rods and cones (*rd/rd cl*) show a marked attenuation in UV sensitivity **(Figure 5B)**. When plotted as EC50 (based on IRC fitting

to individual animals, in all cases R^2>0.89), this is evident as a significant difference in the EC50 (~1.5 log units, P = 1.8x10^{-5}) **(Figure 5C)**. Whilst UV responses are retained following the loss of rods, at the lowest irradiance examined (10.6 log quanta/cm^2/s) a significant attenuation in sensitivity was apparent (P=0.03). This finding suggests that rods are capable of mediating UV responses to low irradiance stimuli. Alternatively, UV cones may be able to mediate low irradiance responses via an interaction with rods, in a similar manner to rods driving entrainment via cones at high irradiances

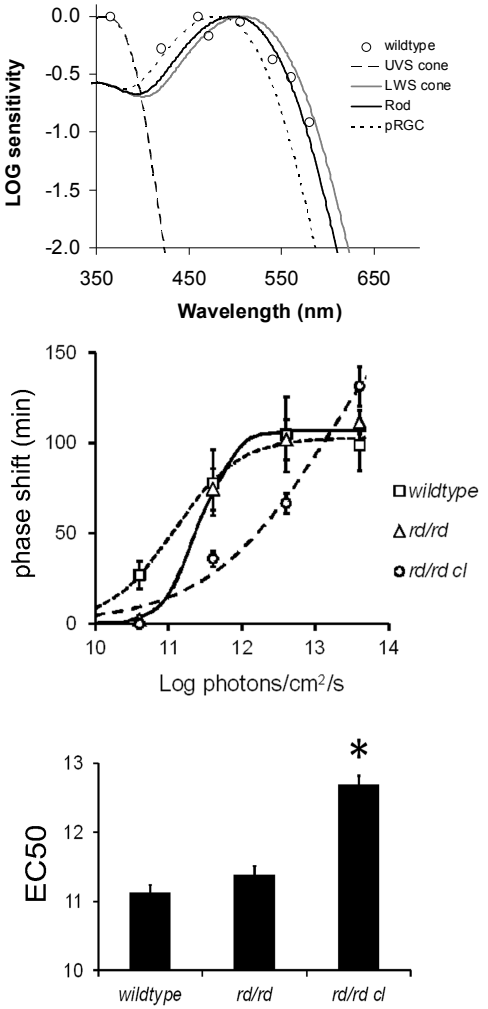

Figure 5. Phase-shifting responses to UV light are cone-dependent. (A) Action spectrum for circadian phase shifting in wildtype mice. Full irradiance response curves were constructed for eight monochromatic wavelengths (365, 420, 460, 471, 506, 540, 560 and 580nm). Action spectrum data are plotted against the known photopigments of the mouse retina (UVS cone λ_{max}=360nm, Opn4 λ_{max}=480, Rod λ_{max} =498nm, LWS cone λ_{max} =508nm). **(B)** Irradiance response curves (IRCs) for phase shifting responses of wildtype C3H, *rd/rd* and *rd/rd cl* to UV light (15 min pulse at CT16, 365 nm UV LEDs). **(C)** Sensitivity to UV was assessed by IRC EC50. Mice lacking rods (*rd/rd*) show no reduction in UV sensitivity compared to wildtype controls. By contrast, mice lacking rods and cones (*rd/rd cl*) show a significantly attenuation of UV sensitivity, with an EC50 1.57 log units higher than controls (P=1.80E-05).

(Altimus et al., 2010). Further studies are obviously required to determine the mechanisms underlying this phenomenon. The residual UV responses in mice lacking rods and cones (*rd/rd cl*) are expected to arise from absorption by the short wavelength limb of the remaining melanopsin photopigment. This would predict a sensitivity of 25% if both α and β absorption peaks contributed, or 4% if this is due to α absorption alone. The measured response of 3% shows that the β absorption peak does not contribute to UV responses (**Figure S6**). These findings are consistent with the role of UVS cones in mediating the influence of UV light on the circadian system.

Conclusion

UV light exposure affects behavioural activity rhythms in an irradiance-, duration- and time-dependent manner. UV light is also as effective as white light in inducing sleep in mice (Lupi et al., 2008). Electrophysiological recordings from the SCN revealed acute responsiveness to UV light exposure. The response was characterized by fast-transient components occurring at the light transitions and a sustained discharge that depends on the level of illumination. This response was preserved in full spectrum saturating white light conditions. Behavioural phase shifting responses, sleep induction and electrical responses to UV light were all preserved in the absence of melanopsin. Critically, mice lacking rods (*rd/rd*) show no attenuation in UV phase shifting responses at medium-high light intensities, whereas mice lacking rods and cones (*rd/rd cl*) show a significant attenuation of UV responses, strongly suggesting these responses are mediated by UVS cones. The present findings show that steady illuminance signalling can occur independently of melanopsin and suggest that UVS cones can play an important role in detecting ambient levels of light. These findings are consistent with a recent study showing a role for UVS cones in pupillary light constriction (Allen et al., 2011). The use of multiple photopigments by mammals may enable the responsiveness to a broad range of wavelengths, and provides sensitivity to subtle differences in the spectral composition of light around dawn and dusk, where there is a relative enrichment of short wavelength light (Hut et al., 2000, Hisdal et al., 2005; Roenneberg and Foster, 1997). UV-sensitivity could therefore contribute to photic entrainment mechanisms particularly in nocturnal animals that operate during the twilight hours.

EXPERIMENTAL PROCEDURES

Animals

Adult male C57BL/6 mice (Harlan, Horst, The Netherlands) (aged 4-12 months) were used to construct behavioral phase and duration response curves for UV-light. Phase shifting studies were performed in male *Opn4*$^{+/+}$ and *Opn4*$^{-/-}$ mice on a C57BL/6 x S129 background (aged 4-8 months). *In vivo* recordings of multiunit activity from the SCN were performed in male C57BL/6 mice (aged 3-12 months) as well as in male *Opn4*$^{+/+}$ and *Opn4*$^{-/-}$ mice (aged 3-6 months). Telemetry studies were performed in male *Opn4*$^{+/+}$ and *Opn4*$^{-/-}$ mice (aged 4-8 months). Adult male *rd/rd* and *rd/rd cl* mice were used to construct the irradiance response curves. All animals were on a C3H background and were 80-100 days old at the beginning of the phase shift experiment. Male C3H wildtype (not carrying the *rd* mutation) controls were age-matched.

Mice were individually housed in cages and isolated from possible confounding external stimuli in light-tight ventilated chambers. Prior to the start of all experiments, mice were entrained to a 12h:12h L:D cycle for a minimum of 14 days. Light onset was designated as Zeitgeber time (ZT) 0 and dark onset as ZT12. Light-dependent resistors connected to a ClockLab interface (Actimetrics, Wilmette, IL, USA) were used to record the light/dark conditions at all times. Ambient temperature was maintained at 20 ± 2 °C and food and water were available *ad libitum*. All aspects of animal work were carried out under Home Office license in accordance with the Animal (Scientific Procedures) Act 1986 (UK), and under the approval of the Animal Experiments Ethical Committee of the Leiden University Medical Centre (The Netherlands).

Circadian activity monitoring

Techniques and protocols for measuring circadian phase shifts to discrete light pulses using the phase of onset of circadian wheel running are well established [54]. Mice were individually housed in cages fitted with running wheels and the presence of wheel-running activity was automatically recorded in 1-min bins by the ClockLab data acquisition system (Actimetrics, Wilmette, IL, USA). Animals were placed in continuous darkness prior to exposure to a phase delaying light pulse. The magnitude of the steady-state behavioral phase shift was determined by fitting straight lines through the activity onsets before and after the light pulse. The difference between the two lines on the day of the light pulse determined the magnitude of the phase shift. Because of transients, the activity onsets on the first three days after the light pulse were excluded from analysis.

Phase response curve and duration response curve to UV light

C57BL/6 mice were entrained to 12:12 LD cycles and released into constant darkness. UV light pulses (365nm; $\lambda_{1/2max}$ 9 nm; 12.9 log quanta/cm^2/s) were applied on the 7th day in DD by transferring the animals to the UV-light set-up within the same room. The phase response curve was constructed from 45 min light pulses applied at different times of the day. The timing of light exposure was calculated based on an animal's individual activity pattern in DD. Following each light pulse, animals were re-entrained to a 12:12 LD cycle before this process was repeated, with a maximum of two light pulses per animal. The duration response curve was constructed from light pulses of different durations (2s, n=4; 10 s, n=6; 100s, n=7; 1000s, n=10; 2700s, n=5; 4000s, n=2; 10000s, n=4) applied at CT14-16 (the time of maximal delays, see **Figure 2B**).

EEG/EMG sleep recordings in Opn4$^{+/+}$ and Opn4$^{-/-}$ mice in response to UV light

To determine if UV light is capable of modulating sleep in the same manner as white light, we also evaluated sleep induction in response to nocturnal UV light exposure. Opn4$^{+/+}$ and Opn4$^{-/-}$ mice anaesthetized under isoflurane (1-3%) were implanted with EEG/EMG telemetry transmitters (TL11M2-F-20, EET, Data Sciences International, St. Paul, USA). Buprenorphrine (Vetergesic 0.015 mg/kg, Alstoe Animal Health, UK) was administered prior to surgery to minimize post-operative pain and temperature was maintained throughout using a heated mat (Habistat, UK). The body of the implant was positioned subcutaneously on the dorsum with EEG electrodes positioned on the cortical surface at following coordinates (1 mm anterior to bregma and 1 mm lateral to the central suture; 3 mm posterior to bregma and 3 mm lateral to the central suture). Electrodes and leads were secured in place using dental adhesive (Reliance, IL, US). EMG electrodes were inserted bilaterally into either side of the musculus cervicoauricularis. Mice were allowed at least 3 weeks to recover before studies were undertaken. All implanted mice remained healthy and gave clear EEG/EMG recordings allowing the discrimination of sleep/wake stages for >4 months. EEG and EMG data were transmitted to a radio receiver (RPC-1, Data Sciences International, St. Paul, USA) placed underneath each cage. Signals were then routed via a data exchange matrix to a PC running Dataquest A.R.T. software (version 3.01). The EEG and EMG data were continuously sampled using DSI Dataquest Gold acquisition software (DSI) at 500 Hz, with a 100 Hz filter cut-off. EEG and EMG signals were band-pass filtered (0.5-35 Hz for EEG and 80-100 Hz for EMG) and sleep/wake stages were scored offline as wakefulness, non-rapid eye movement (NREM) sleep and rapid eye movement (REM) sleep in 10 sec epochs using a semi-automated approach. The sleep scoring procedure consisted an initial automated step using

SleepSign® software (Kissei Comtec, Nagano, Japan), followed by a review of all epochs by an experienced sleep scorer. During a baseline period (day 1) *Opn4*$^{+/+}$ and *Opn4*$^{-/-}$ mice implanted with EEG/EMG telemetry transmitters housed in a light tight chamber were left undisturbed in the usual light/dark conditions. On the following day (day 2), a 1-hour 363nm light pulse was administered at ZT16. EEG and EMG were recorded continuously for a period of four hours from ZT14-ZT18 on both experimental days. Time course analysis and the total NREM and REM sleep were calculated for the 1 hour light pulse vs. the 1-hour sham period for each genotype.

Statistical Analysis

Statistical analysis was performed using GraphPad Prism software (GraphPad) or OriginV7 software (OriginLab, Northampton USA). Significant differences between groups were determined using either two-tailed unpaired Student's t-test or one-way ANOVA, followed by Bonferroni's *post-hoc* test. Values were considered significantly different where $p < 0.05$.

Electrophysiology Recordings

Procedures for *in vivo* recordings of multiunit activity (MUA) from SCN neurons have been described previously (Meijer et al., 1998). Using a stereotactic instrument, tripolar stainless steel micro-electrodes (Plastics One, USA) were implanted in mice (minimum age 12 weeks, 20-30 gram) under Hypnorm/Dormicum anesthesia. Two twisted electrodes (Polyimide-insulated; bare electrode diameter 0.125 mm) for differential recording were aimed at the SCN (coordinates: 0.46 mm posterior to bregma, 0.14 mm lateral to the midline, 5.2 mm ventral to the surface of the cortex, under a 5-degree angle in the coronal plane (Paxinos and Franklin, 2001), and a third uncoated reference electrode was placed in the cortex. After recovery, the animals were connected to the recording system with a counterbalanced swivel system enabling the animals to move freely during the measurements. The electrical signal was amplified and bandwidth filtered (0.5 - 5kHz). Window discriminators were used to convert action potentials into digital pulses that were counted in 2 sec epochs (CircaV1.9 custom made software) and stored for offline analysis.

To obtain uniform illumination levels, recordings were performed in a half-sphere (diameter 30 cm) coated with high reflectance paint (Barium Sulphate; Labsphere WRC-680). At the top of the sphere an opening (diameter 5 cm) was created for the connecting swivel system. The sphere was illuminated by monochromatic UV light using high power LEDs (NCCU033, Nichia, Japan) positioned in a circle at the upper part of the sphere, and a baffle prevented the animal from looking directly into the

light. Within the sphere a UV-transparent perspex cylinder was used to house the animal. The actual wavelength and light irradiances were measured at a fixed position on the floor of the cage using a calibrated spectrometer (AvaSpec2048, Avantes, The Netherlands). Irradiance levels were manually regulated using a current source and the timing of the applied light pulses was computer controlled. All light pulses were applied against a dark background. The actual wavelength was 365 nm and half-maximal bandwidth ($\lambda_{1/2}$) was 9 nm. To characterize the electrical response pattern of the SCN, UV light pulses of various durations (ranging from 2 sec to 10 min at constant irradiance of 12.9 log quanta/cm^2/s) and intensities (ranging from 11 to 13 log quanta/cm^2/s; 100 sec pulses) were applied between CT14-16. The absolute magnitude of light responses between animals was different, due to differences in spike recording settings and/or differences in recording location within the SCN (i.e. highly innervated versus less innervated area). For the quantification of irradiance responses, mean changes in discharge rate as compared to baseline levels were calculated. The baseline level was defined as the average firing rate of the last 100 sec before lights on, the transient on-excitation discharge level was determined by the firing rate of the first 2 sec epoch after lights on, and the steady state discharge level was quantified as the average firing rate during the entire period of light exposure (excluding the first 50 sec due to the transient response). To investigate responsiveness of the SCN to UV light as a function of circadian time, 5-min light pulses of constant irradiance (12.9 log quanta/cm^2/s) were applied every hour. The circadian time of the light responses was calculated per day on the basis of the onset of behavioral activity as recorded by a passive infrared sensor.

To investigate the responses to the light pulses in more detail, the electrophysiological signals of SCN activity were digitized at 25 kHz using Spike2 hardware and software (Cambridge Electronic Design) and stored for off-line analysis. The digitized recordings were imported into MATLAB as 'waveform data', including data from light and movement sensors, using parts of the sigTOOL SON Library (http://sigtool.sourceforge.net). Imported waveform data were triggered at fixed voltage amplitude settings, and time and amplitude of these action potentials were used for the analysis. To investigate the latency of the neuronal response to light onset, digitized action potentials were counted in 0.01s bins. For a detailed analysis of population activity, a baseline recording (100s before light pulse) was used to create a spike amplitude histogram. On the basis of this amplitude histogram, thresholds were set in such a way that the average number of counts within each threshold window was equal. Threshold windows were non-overlapping and started above noise level. Action potentials were counted within each step of set thresholds

for the remainder of the recording. The measurement of SCN sub-populations on the basis of baseline electrical activity levels leaves the neuronal response after baseline as a free parameter (see Vanderleest et al., 2009), and enables comparisons between different, approximately equal-sized, populations of neurons. The use of these datasets provides insight into firing responses of small populations of cells. Action potentials were counted in 1s bins.

Histology

At the end of each recording, tissue was collected for the purpose of histological verification of the electrode location. The recording site was marked by passing a small electrolytic current through the electrode to deposit iron at the electrode tip, which was stained blue by immersing the brain in a potassium ferrocyanide containing fixative solution. The brain was sectioned coronally and stained with neutral red for microscopic reconstruction of the recording site. Recordings from outside the SCN were excluded from the final analysis.

UV Irradiance response curves

All control C3H, *rd/rd* and *rd/rd cl* were entrained to 12/12 LD then placed in DD for 2 weeks prior to the initial UV light pulse. Light pulses at 365 nm were given weekly for 15 minutes in a separate pulsing chamber at CT16 using a custom-made light source consisting of 5 UV LEDs (NCCU033, Nichia, Japan). Excel (Microsoft) was used to fit a four parameter sigmoid curve based upon the method of least squares, as described previously (Peirson et al., 2005, Meth Enzymology).

Acknowledgments

We thank Prof. Mark Hankins for his advice on UV photoreceptor biology. We thank Dr. Christiana Katti for assistance with genotyping the *Opn4* animals. We thank Hans Duindam for assistance with animal handling and surgery, Peter Stouten for support in histology procedures, and Nico de Haas, Bram de Visser, Jan Janse and Sander van Berloo for technical support in designing and building the experimental light set-up and recording system. The work leading to this paper has been supported by a grant to RGF, SNP and JHM from the Wellcome Trust, and to JHM/RGF from the EC FP6 integrated project 'EUCLOCK' (contract number 018741).

REFERENCES

Aggelopoulos, N.C. and Meissl, H. (2000). Responses of neurons of the rat suprachiasmatic nucleus to retinal illumination under photopic and scotopic conditions. J. Physiol. *1*, 211-222.

Allen, A.E., Brown, T.M., Lucas, R.J. (2011). A distinct contribution of short-wavelength-sensitive cones to light-evoked activity in the mouse pretectal olivary nucleus. J. Neurosci. *31*, 16833-16843.

Altimus, C.M., Güler, A.D., Alam, N.M., Arman, A.C., Prusky, G.T., Sampath, A.P., and Hattar, S. (2010). Rod photoreceptors drive circadian photoentrainment across a wide range of light intensities. Nat. Neurosci. *13*, 1107-1112.

Altimus, C.M., Güler, A.D., Villa, K.L., McNeill, D.S., Legates, T.A., and Hattar, S. (2008). Rods-cones and melanopsin detect light and dark to modulate sleep independent of image formation. Proc. Natl. Acad. Sci. U. S. A. *105*, 19998-20003.

Amir, S. and Robinson, B. (1995). Ultraviolet light entrains rodent suprachiasmatic nucleus pacemaker. Neuroscience *69*, 1005-1011.

Belenky, M.A., Smeraski, C.A., Provencio, I., Sollars, P.J., and Pickard, G.E. (2003). Melanopsin retinal ganglion cells receive bipolar and amacrine cell synapses. J. Comp. Neurol. *460*, 380-393.

Benshoff, H.M., Brainard, G.C., Rollag, M.D., and Lynch, G.R. (1987). Suppression of pineal melatonin in Peromyscus Leucopus by different monochromatic wavelengths of visible and near-ultraviolet light (UV-A). Brain Res. *420*, 397-402.

Berson, D.M., Dunn, F.A., and Takao, M. (2002). Phototransduction by retinal ganglion cells that set the circadian clock. Science *295*, 1070-1073.

Brainard, G.C. Barker, F.M., Hoffman, R.J., Stetson, M.H., Hanifin, J.P., Podolin, P.L., and Rollag, M.D. (1994). Ultraviolet regulation of neuroendocrine and circadian physiology in rodents. Vision Res. *34*, 1521-1533.

Brown, T.M., Wynne, J., Piggins, H.D., and Lucas, R.J. (2011). Multiple hypothalamic cell populations encoding distinct visual information. J. Physiol. *589*, 1173–1194.

Dacey, D.M., Liao, H.W., Peterson, B.B., Robinson, F.R., Smith, V.C., Pokorny, J., Yau, K.W., and Gamlin, P.D. (2005). Melanopsin-expressing ganglion cells in primate retina signal colour and irradiance and project to the LGN. Nature *433*, 749-754.

Drouyer, E., Rieux, C., Hut, R.A., and Cooper, H.M. (2007). Responses of suprachiasmatic nucleus neurons to light and dark adaptation: relative contributions of melanopsin and rod-cone inputs. J. Neurosci. *27*, 9623-9631.

Gooley, J.J., Rajaratnam, S.M., Brainard, G.C., Kronauer, R.E., Czeisler, C.A., and Lockley, S.W. (2010). Spectral responses of the human circadian system depend on the irradiance and duration of exposure to light. Sci. Transl. Med. *2*, 31ra33.

Göz, D., Studholme, K., Lappi, D.A., Rollag, M.D., Provencio, I., and Morin, L.P. (2008) Targeted destruction of photosensitive retinal ganglion cells with a saporin conjugate alters the effects of light on mouse circadian rhythms. PLoS One. *3*, e3153.

Groos, G.A. and Mason, R. (1980). The visual properties of rat and cat suprachiasmatic neurons. J. Comp. Physiol. *135*, 349-356.

Güler, A.D., Ecker, J.L., Lall, G.S., Haq, S., Altimus, C.M., Liao, H.W., Barnard, A.R., Cahill, H., Badea, T.C., Zhao, H., et al. (2008). Melanopsin cells are the principal conduits for rod-cone input to non-image-forming vision. Nature *453*, 102-105.

Hatori, M., Le, H., Vollmers, C., Keding, S.R., Tanaka, N., Buch, T., Waisman, A., Schmedt, C., Jegla, T. and Panda, S. (2008) Inducible ablation of melanopsin-expressing retinal ganglion cells reveals their central role in non-image forming visual responses. PLoS One. *3*, e2451.

Hisdal, V. (2005) On the Relative Spectral Distribution of the Radiation from the Zenith Sky. Theoretical and Applied Climatology *10*, 59-68.

Hut, R.A., Scheper, A., and Daan, S. (2000). Can the circadian system of a diurnal and a nocturnal rodent entrain to ultraviolet light? J. Comp. Physiol. *186*, 707-715.

Lall, G.S., Revell, V.L., Momiji, H., Al Enezi, J., Altimus, C.M., Güler, A.D., Aguilar, C., Cameron, M.A., Allender, S., Hankins, M.W., and Lucas, R.J. (2010). Distinct contributions of rod, cone, and melanopsin photoreceptors to encoding irradiance. Neuron *13*, 66417-66428.

Lupi, D., Oster, H., Thompson, S., and Foster, R.G. (2008). The acute light-induction of sleep is mediated by OPN4-based photoreception. Nat. Neurosci. *11*, 1068-1073.

Meijer, J.H., Groos, G.A., and Rusak, B. (1986). Luminance coding in a circadian pacemaker: the suprachiasmatic nucleus of the rat and the hamster. Brain Res. *382*, 109-118.

Meijer, J.H., Rusak, B., and Gänshirt, G. (1992). The relation between light-induced discharge in the suprachiasmatic nucleus and phase shifts of hamster circadian rhythms. Brain Res. *598*, 257-263.

Meijer, J.H., Watanabe, K., Schaap, J., Albus, H., and Détári, L. (1998). Light responsiveness of the suprachiasmatic nucleus: long-term multiunit and single-unit recordings in freely moving rats. J. Neurosci. *18*, 9078-9087.

Mure, L.S., Rieux, C., Hattar, S., and Cooper, H.M. (2007). Melanopsin-dependent nonvisual responses: evidence for photopigment bistability in vivo. J. Biol. Rhythms *22*, 411-424.

Nelson, D.E. and Takahashi, J.S. (1999). Integration and saturation within the circadian photic entrainment pathway of hamsters. Am. J. Physiol. *277*, R1351-1361.

Paxinos, G. and Franklin, K.B.J. (2001). The mouse brain in stereotaxic coordinates (San Diego: Academic Press, 2nd edition)

Pittendrigh, C.S. and Daan, S. (1976). A Functional Analysis of Circadian Pacemakers in Nocturnal Rodents: II. The Variability of Phase Response Curves. J. Comp. Physiol. *106*, 253-266.

Podolin, P.L., Rollag, M.D., and Brainard, G.C. (1987). The suppression of nocturnal pineal melatonin in the Syrian hamster: dose-response curves at 500 and 360 nm. Endocrinology *121*, 266-270.

Provencio, I. and Foster, R.G. (1995). Circadian rhythms in mice can be regulated by photoreceptors with cone-like characteristics. Brain Res. *694*, 183-190.

Roenneberg, T. and Foster, R.G. (1997). Twilight times: light and the circadian system. J. Photochem. Photobiol. *66*, 549-561.

Schmidt, T.M. and Kofuji, P. (2010). Differential cone pathway influence on intrinsically photosensitive retinal ganglion cell subtypes. J. Neurosci. *30*, 16262-16271.

Sekaran, S., Foster, R.G., Lucas, R.J., and Hankins, M.W. (2003). Calcium imaging reveals a network of intrinsically light-sensitive inner-retinal neurons. Curr Biol. *13*, 1290-1298.

Sharma, V.K., Chandrashekaran, M.K., Singaravel, M., and Subbaraj, R. (1998). Ultraviolet-light-evoked phase shifts in the locomotor activity rhythm of the field mouse Mus booduga. J. Photochem. Photobiol. *45*, 83-86.

Sharma, V.K., Chidambaram, R., Singh, T.J., Lingakumar, K., Subbaraj, R. and Chandrashekaran, M.K. (2000). Irradiance dependency of UV-A induced phase shifts in the locomotor activity rhythm of the field mouse Mus booduga. Chronobiol. Int. *17*, 777-782.

Tsai, J.W., Hannibal, J., Hagiwara, G., Colas, D., Ruppert, E., Ruby, N.F., Heller, H.C., Franken, P., and Bourgin, P. (2009). Melanopsin as a sleep modulator: circadian gating of the direct effects of light on sleep and altered sleep homeostasis in Opn4(-/-) mice. PLoS Biol. *7*, e1000125.

VanderLeest, HT., Rohling, J.H., Michel, S. and Meijer, J.H. (2009). Phase shifting capacity of the circadian pacemaker determined by the SCN neuronal network organization. PLoS One *4*, e4976.

Von Schantz, M., Argamaso-Hernan, S.M., Szél, A., and Foster R.G. (1997). Photopigments and photoentrainment in the Syrian golden hamster. Brain Res. *770*, 131-138.

Wong, K.Y., Dunn, F.A., Graham, D.M., and Berson, D.M. (2007). Synaptic influences on rat ganglion-cell photoreceptors. J. Physiol. *582*, 279-296.

SUPPLEMENTARY FIGURES

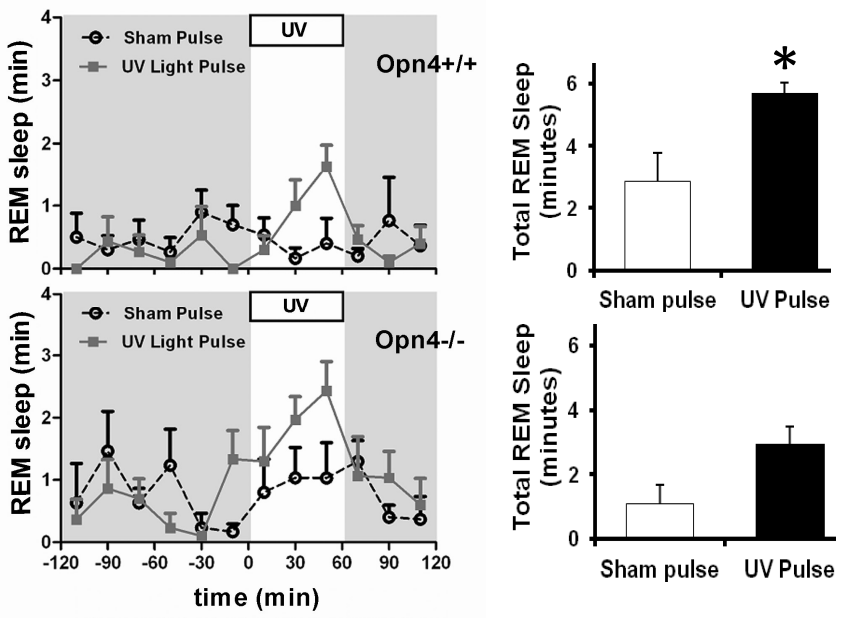

Supplementary Figure 1. UV light-induced REM sleep in *Opn4+/+ and Opn4-/-* mice. (A) Time course of REM sleep following UV light exposure, showing responses in $Opn4^{+/+}$ and $Opn4^{-/-}$ mice (n=5). **(B)** Histograms summarizing changes in REM sleep in response to UV light exposure. UV light administered at ZT 16-17 results in a significant increase of REM sleep in $Opn4^{+/+}$ mice. Whilst REM sleep also appeared to increase in $Opn4^{-/-}$ animals, this was not statistically significant. * indicates P<0.05.

Supplementary Figure 2. Electrical activity from SCN sub-populations. Representative examples of electrical activity as recorded simultaneously from two SCN sub-populations. Action potential thresholds were set off-line in such a way that an average firing frequency of 130Hz was measured during baseline, in order to obtain approximately equal-sized populations of neurons. Upper graph: threshold window was set from -1.2 to -1.3V. Lower graph: threshold window was set from -1.7 to -1.9V. During the light pulse, spikes between set thresholds were counted, and revealed that the increased firing rate in response to UV light is not present in some neurons (upper graph), while it is apparent in others (lower graph). Bin size is 1s. Stimulus presentation is indicated by the step diagram above the plot.

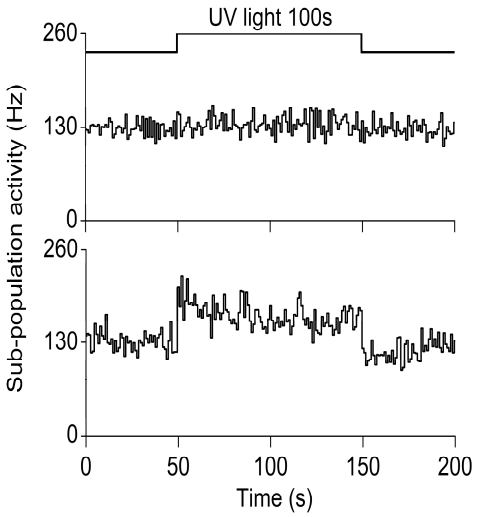

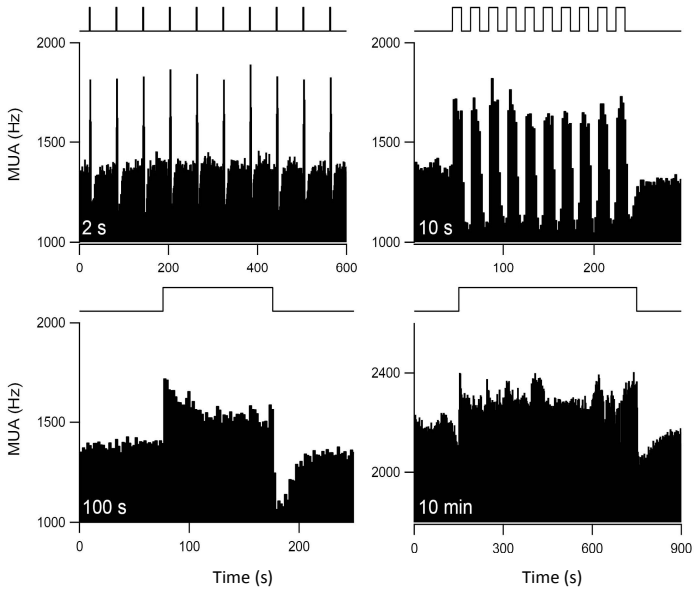

Supplementary Figure 3. SCN electrical responses to UV light pulses of different durations in melanopsin - deficient (*Opn4*$^{-/-}$) mice. Upper left: 2s lights on, 58s lights off (10x); Upper right: 10s lights on, 10s lights off (10x); Lower left: 100s lights on; Lower right: 10 min lights on. Bin size is 2s. MUA = multi-unit activity. Stimulus presentation is indicated by the step diagram above each plot.

Supplementary Figure 4. Type II phase-shifting responses to 360nm (UV) light in *Opn4*$^{+/+}$ and *Opn4*$^{-/-}$ mice. *Opn4*$^{+/+}$ and *Opn4*$^{-/-}$ mice were maintained under a light/dark cycle of 12h/12h (L:D 12:12) with free access to running wheels. Once fully entrained, mice were exposed to a 15-min light pulse of UV light (11.8 log quanta/cm2/s) at Zeitgeber Time 14 (n =9 per genotype). After the pulse, mice were placed in constant darkness for an additional 10 days to determine the phase shift in behavioral activity. Exposure to UV light produced an equivalent phase delay in Opn4+/+ and Opn4-/- mice. Data are presented as mean values (± SEM).

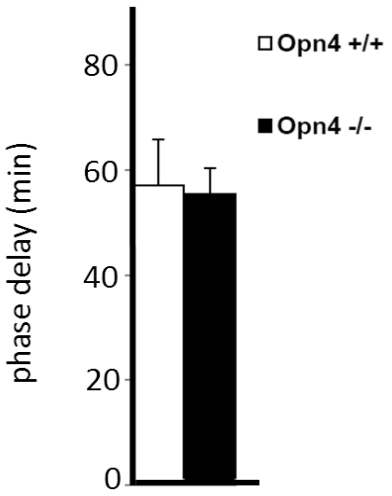

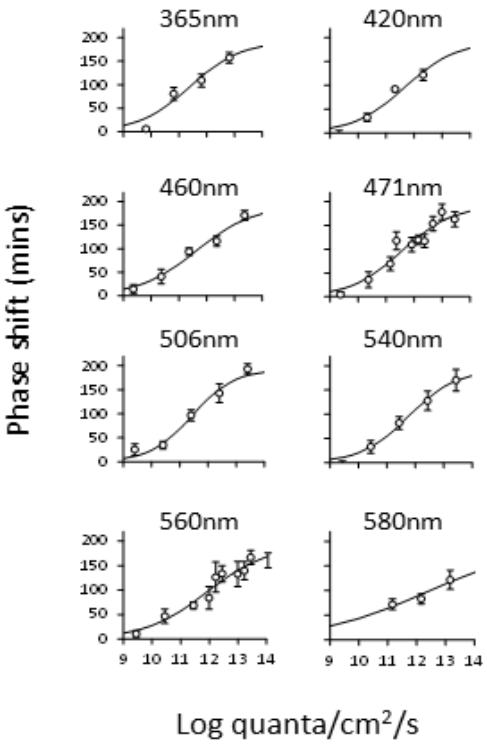

Supplementary Figure 5. Irradiance response curves (IRCs) for phase-shifting responses in wildtype mice over a range of wavelengths. The relationship between irradiance and phase shift magnitude (mean and standard error) is fitted with a variable slope sigmoid dose response function. Maximum phase shift obtained was 192.1mins. These IRCs were used to generate a wildtype action spectrum (**Figure 4A**) at eight monochromatic wavelengths: 365, 420, 460, 471, 506, 540, 560 and 580nm.

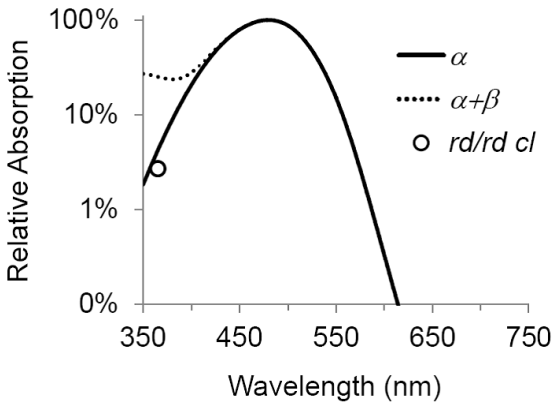

Supplementary Figure 6. Phase-shifting responses in the absence of rods and cones. The residual UV responses in mice lacking rods and cones (*rd/rd cl*) may arise from absorption by the short wavelength limb of the remaining melanopsin cells in this mouse model. A 480nm photopigment template was plotted including α and β absorption peaks or α absorption peak alone. This would predict a sensitivity of 25% if both α and β absorption peaks contributed to UV responses, or 4% is this is due to α absorption alone. The measured response of 3% strongly suggests that the β absorption peak does not contribute to residual UV responses in *rd/rd cl* animals.